

COMPARATIVE STUDY ON DIFFERENT HIS AS GROUND PLANES AND ITS APPLICATION TO LOW PROFILE WIRE ANTENNAS DESIGN

I. Tomeo-Reyes

Department of Electronic Technology
University Carlos III of Madrid, Spain

E. Rajo-Iglesias

Department of Signal Theory and Communications
University Carlos III of Madrid, Spain

Abstract—In this paper, the characteristics of three different types of high impedance surfaces (HIS) to be used as ground planes for low profile wire antennas are investigated and compared: a mushroom-like surface, which is the classical example of HIS with connecting vias, and two surfaces with no vias, one of which is anisotropic. Both the simulation results and the measurements verify that the high impedance behaviour is successfully accomplished around the resonant frequency. In order to complete the study, return loss and radiation pattern of a horizontal dipole placed above the surfaces are analyzed.

1. INTRODUCTION

Artificial electromagnetic materials, also known as metamaterials, are periodic electromagnetic structures with properties impossible to find in natural materials. Such properties, led to a wide range of applications in the electromagnetism field. Remarkable metamaterial structures are, for example, double negative (DNG) [1, 2], electromagnetic band gap (EBG) structures [3], double zero metamaterials (DZR) [4] or zero-index (ZIM) and near-zero-index (NZIM) metamaterials [5].

When working with metamaterials, the reflected electric field phase, or simply reflection phase, is of special interest because it is

Received 28 January 2011, Accepted 15 March 2011, Scheduled 19 March 2011

Corresponding author: Inmaculada Tomeo-Reyes (itomeo@ing.uc3m.es).

the way to distinguish perfect electric conductors (PEC) from perfect magnetic conductors (PMC). When a plane wave normally illuminates a PEC surface, the phase of the reflected field at its surface is 180° . If this occurs with a PMC surface, such phase will be 0° . When working with surfaces with a reflection phase equal or near 0° , it is common to talk about artificial magnetic conductor (AMC), instead of PMC, as pure PMC surfaces cannot be found in nature. Another interesting characteristic of metamaterials is that some of them have a forbidden frequency band, usually known as electromagnetic band gap (EBG), in which no surface wave can propagate along the surface. High impedance surfaces may show the two interesting behaviours just mentioned: AMC and EBG. Moreover, depending on the geometry of the unit cell used to implement the surface, both behaviours may appear in the same frequency range [6, 7].

AMC behaviour occurs because HIS have very high impedance in a specific frequency range, range in which the tangential component of the electric field is small. For this reason, these surfaces reflect the incident waves with a phase equal or near 0° . In practice, the reflection phase of HIS varies continuously from 180° to -180° versus frequency, and takes zero value just at one frequency. This fact is fundamental when considering low profile wire antenna design, as the parallel image currents appear in-phase, rather than out-of-phase, and so, efficient radiation for antennas placed parallel and close to the surface is possible [8]. Different experimental ways of characterizing the AMC behaviour can be considered [9, 10].

On the other hand, due to the special periodic structure of HIS, they show an effective EBG for surface-wave propagation, which can be useful to improve antenna radiation patterns [11–13]. When avoided the surface waves, there is an absence of multipath and radiation patterns are smoother.

The different topologies that can be considered when implementing HIS, share the same basic structure. Such structure is periodically repeated and basically consists of a metallization printed on a grounded dielectric slab. The presence or absence of metallic vias to connect the metallization to the ground also depends on the specific topology. Considering both the influence of the type of metallization and the fundamental role of the via for tailoring the AMC and EBG behaviour, the three surfaces that have been chosen to be studied are the mushroom-like surface, which is the classical example of HIS with connecting vias, the ring metallization HIS, with no via, and the open ring metallization HIS, which has no via either and is anisotropic. Unlike the ring-shaped metallization structures, the reference structure (mushroom-like), has been extensively studied in literature (see Fig-

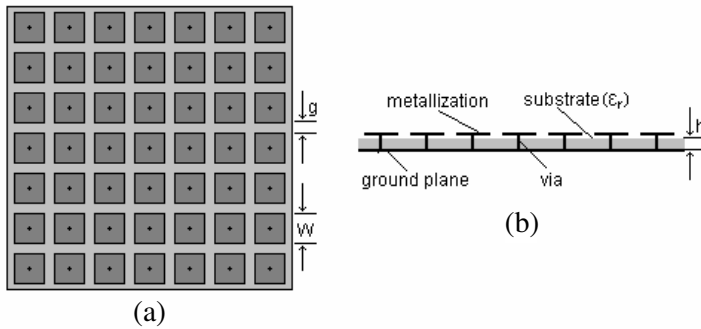


Figure 1. Mushroom-like surface. (a) Top view and (b) side view.

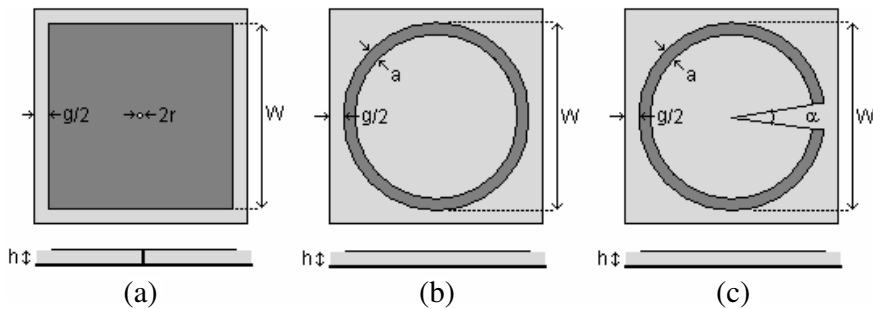


Figure 2. (a) Mushroom-like cell, (b) ring metallization cell and (c) open ring metallization cell.

ure 1) [14, 15]. For this reason, special attention has been paid when studying the behaviour of both the ring and open ring metallization structures.

2. UNIT CELL DESIGN

Considering the usefulness of HIS as ground planes, and with the aim of obtaining design guidelines, it is necessary to characterize such surfaces by performing parametric studies of the unit cell.

2.1. AMC Behaviour Analysis

According to the introduction, three different surfaces are going to be analysed: mushroom-like, ring metallization and open ring metallization HIS. The unit cells that correspond to each of them are shown in Figure 2, being the design parameters of the cells:

metallization width (W), gap width (g), substrate permittivity (ε_r) substrate thickness (h), ring width (a) and open sector size (α). The starting design parameters, using the free space wavelength at 2 GHz as a reference length and fixing the unit cell size (period), are as follows:

$$\begin{aligned} W &= 0.17\lambda_{2\text{GHz}}, & g &= 0.013\lambda_{2\text{GHz}}, & \varepsilon_r &= 2.2, & h &= 0.025\lambda_{2\text{GHz}}, \\ r &= 0.0017\lambda_{2\text{GHz}}, & a &= 0.007\lambda_{2\text{GHz}}, & \alpha &= 5^\circ \end{aligned} \quad (1)$$

In order to determine the AMC behaviour of the different unit cells, a normally incident plane wave is considered. The reflection phase is then measured.

Figure 3 shows the reflection phase of the three different unit cells. As expected, mushroom-like and ring metallization structures, both of them symmetric, have the same reflection phase for x and y polarizations. This is not the same in the case of the open ring metallization structure, in which the reflection phase behaviour varies considerably depending on the polarization due to its asymmetry.

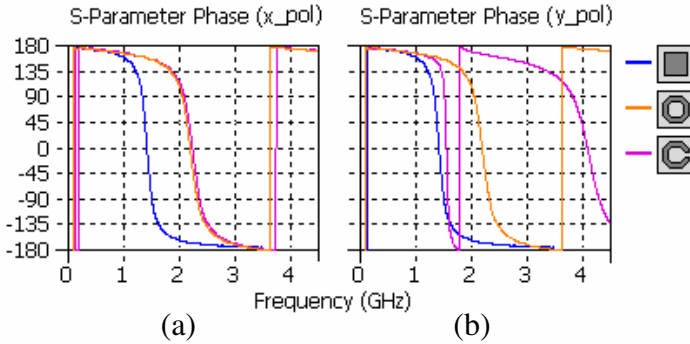


Figure 3. Reflection phase of the three different unit cell geometries. (a) Incident wave x -polarized and (b) incident wave y -polarized.

Another significant point to notice is that, according to the results obtained when the incident wave is x -polarized (Figure 3(a)), the most compact structure is the mushroom-like one, because, having the same dimensions as the other ones, its AMC behaviour is reached at a lower frequency. This is equivalent to say that for the same frequency value, its size is the smallest. This behaviour is essentially due to the high capacitance between the periodic metallic patches. The effect of the vias in this case is negligible, and the same reflection phase is obtained in the cases with and without vias, as already demonstrated in [6, 16]. Regarding the ring-shaped metallization structures, the open ring cell is more compact than the ring one (see Figure 3(b)).

In order to choose which structure is the most appropriate to implement a ground plane for low profile wire antennas, it will be

necessary to determine the antenna characteristics (return losses and radiation diagram) in each case.

2.2. Unit Cell Parametric Study

Apart from the metallization shape, the reflection phase in the case of AMC surfaces is basically determined by four parameters (see Figure 2): metallization width (W), gap width (g), substrate permittivity (ϵ_r) and substrate thickness (h); or five, including ring width (a), when working with ring-shaped metallization unit cells.

In order to perform the parametric study of the different unit cells, a normally incident plane wave is considered. The reflection phase is then measured while varying the value of the different parameters. To analyse the AMC behaviour of the three structures considering the influence of the cell main parameters, the frequency at which the reflection phase is zero has to be analyzed. Figure 4 shows the zero-reflection-phase frequency values obtained when varying the structures main parameters.

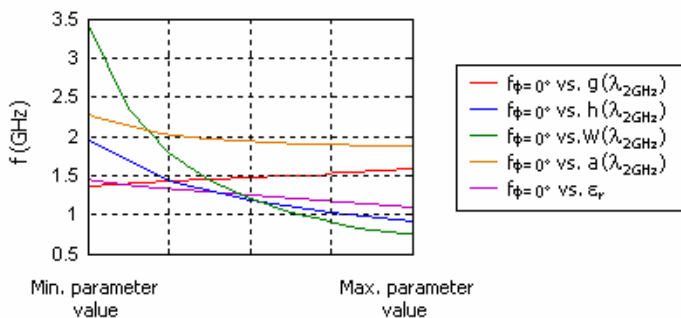


Figure 4. Frequency value when reflection phase is zero vs. HIS characteristic parameters. Values of g , h , W and ϵ_r correspond to mushroom-like cell, but the behaviour is the same in the cases of both ring-shaped cells. Values of ring width, a , correspond to the ring metallization cell, but are also valid in the case of the open ring cell.

It is also important to notice that, apart from the four/five main parameters, there are other minor parameters to consider, as vias radius (r) and position in the case of the mushroom-like cell, and open sector size (α) in the case of the open ring metallization unit cell. The influence of these parameters has been checked not to be very determining as the variation in all cases is quite linear and plane.

According to the results, the frequency variation is decreasing for all parameters except the gap width. This means that the frequency in which the reflection phase is 0° , increases when all parameters, except the gap, decrease.

The variation of frequency versus gap width, substrate permittivity and ring width is almost linear, being the slope quite small. On the contrary, variation versus metallization width and substrate thickness is quadratic, and the frequency range is quite bigger. This information indicates that metallization width and substrate thickness are the parameters that most affect the frequency value in which the reflection phase is zero. Nevertheless, being the variation quadratic, when the value of such parameters is small, the frequency variation is quite big, but once reached certain value, it hardly changes. This way, it has no sense to increase the value of both parameters as much as desired, because no effect will be noticed.

3. HI GROUND PLANES CHARACTERIZATION

To completely characterize the three ground planes we are going to work with, both AMC and EBG behaviour will be analyzed. As previously commented, depending on the geometry of the unit cell used to implement the high impedance surface, both behaviours may appear in the same frequency range.

Figure 2 shows the geometry of the three different unit cells, where the spacing between them, g , was determined as 2 mm. All metallizations are printed on a polyethylene substrate with dielectric constant of 2.2, loss tangent of 0.0004 and thickness of $0.033\lambda_{2\text{GHz}}$ (5 mm). The radius of the metallic via of the mushroom is $r = 0.0017\lambda_{2\text{GHz}} = 0.25$ mm and, in the case of the rings, $a = 0.013\lambda_{2\text{GHz}} = 2$ mm and $\alpha = 10^\circ$. Only the width (period of the unit cell) is different in all cases, so that the frequency in which the reflection phases for all three cases are 0° can be fixed to the same value. Using a simulation tool (CST Microwave Studio) all surfaces have been designed to include in-phase reflection on their surfaces for a normally incident plane wave at 2 GHz. In order to fix the resonant frequency to 2 GHz, the metallization width in each case must be, respectively, $0.133\lambda_{2\text{GHz}}$, $0.193\lambda_{2\text{GHz}}$ and $0.14\lambda_{2\text{GHz}}$ (20, 29 and 21 mm). This result indicates that the most compact structure is the mushroom-like one, as previously mentioned. Once known the size of each basic structure, the number of cells per dimension needed to implement each ground plane must be decided. In this case, to make the dimensions of all planes as similar as possible, and in order to avoid excessively big ground planes, $N = 8, 5$ and 7 has been respectively chosen.

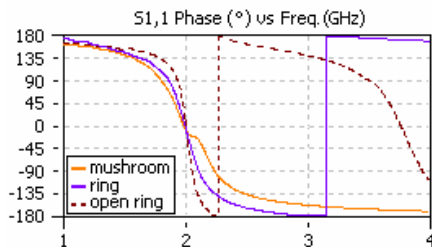


Figure 5. Simulated reflection phase of the HIS-based ground planes.

Once the ground planes are completely designed, AMC and EBG behaviours can be analysed. In order to characterize the AMC behaviour, the reflection phase of the three planes is studied (see Figure 5). According to the results shown in Figure 5, for a frequency value of 2 GHz, in-phase reflection is observed in all cases. Furthermore, variation with frequency is faster in the case of the rings. Regarding the EBG behaviour, it has been proved, via simulation of the dispersion diagrams, that the mushroom-like plane shows a very noticeable EBG in the 1.5–2.4 GHz frequency band. In this case, both the AMC and the EBG behaviour occur in the same frequency range, something very positive taking into account that at 2 GHz, apart from the fact that in-phase reflection exists, surface waves suppression is achieved. The presence of vias is the determinant fact for this to occur. In the case of the ring-shaped metallization planes, no EBG behaviour is observed.

4. HORIZONTAL DIPOLE OVER HI GROUND PLANE

Normally, when above a conventional metallic ground plane, horizontal wire antennas radiate very poorly as the image currents appear out-of-phase, rather than in-phase and cancel the currents in the antenna. This situation improves when using a HIS as a ground plane. The horizontal dipole has been analyzed in order to confirm this fact.

When designing an antenna in conjunction with a HIS, it must be taken into account that both elements must be designed simultaneously, as a single antenna structure. The design methodology consists of three basic steps. First of all, as explained in detail in Sections 2 and 3, the unit cell and plane are designed in order to set the resonant frequency to the desired value, 2 GHz in this case. Secondly, a reference half-wave dipole is located at a fixed height. Normally, heights between 2 and 10 mm make the structure work correctly, although it is more complicated to obtain good return loss when

Table 1. High impedance ground plane dimensions[†].

Metallization	Width
Mushroom	$0.113\lambda_{2\text{GHz}} = 17.06 \text{ mm}$
Ring	$0.211\lambda_{2\text{GHz}} = 31.6 \text{ mm}$
Open Ring	$0.13\lambda_{2\text{GHz}} = 19.5 \text{ mm}$

Table 2. Horizontal dipole dimensions.

Metallization	Length	Height
Mushroom	$0.50\lambda_{2\text{GHz}} = 75 \text{ mm}$	$0.047\lambda_{2\text{GHz}} = 7 \text{ mm}$
Ring	$0.40\lambda_{2\text{GHz}} = 60 \text{ mm}$	$0.047\lambda_{2\text{GHz}} = 7 \text{ mm}$
Open Ring	$0.60\lambda_{2\text{GHz}} = 90 \text{ mm}$	$0.047\lambda_{2\text{GHz}} = 7 \text{ mm}$

working in the interval edges. Finally, by gradually varying the dipole length, the optimal size of the antenna is calculated via simulation tool (CST Microwave Studio). Considering the high influence the antenna has in the HIS behaviour, it can happen that the desired resonant frequency is not obtained by only varying the dipole length. In this case, the unit cell metallization size (W), which is the most influential parameter according to Section 2.2 results, is readjusted considering that in order to increase the frequency, W must decrease, and viceversa.

The definitive dimensions of both the HIS metallization and the horizontal dipole in all three cases under study are shown in Tables 1 and 2 respectively.

Once defined both the ground planes and the horizontal dipoles, return loss and radiation pattern in all cases must be analysed.

4.1. Mushroom-like Ground Plane (8×8 Unit Cells)

The first structure to be studied is the one made of a horizontal dipole over a mushroom-like HIS (see Figure 6).

First, the simulated return loss will be analysed, comparing the result with the cases with PEC ground plane and no ground plane (see Figure 7(a)).

As expected, when the horizontal dipole is over a PEC ground plane, due to image theory, it is not matched. On the contrary, when the dipole is in free space, with no ground plane, return loss is quite good. A priori, this can be considered a great advantage; however, there are applications in which a ground plane is compulsory. It is precisely in these cases that the HIS based ground plane is needed,

[†] Parameters different from width remain the same as stated in Section 3.

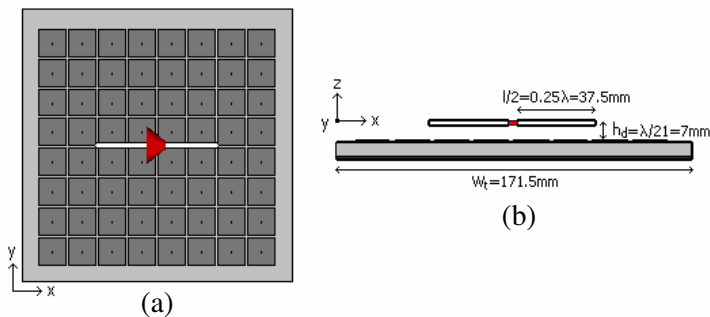


Figure 6. Horizontal dipole over mushroom-like HIS. (a) Top view and (b) side view.

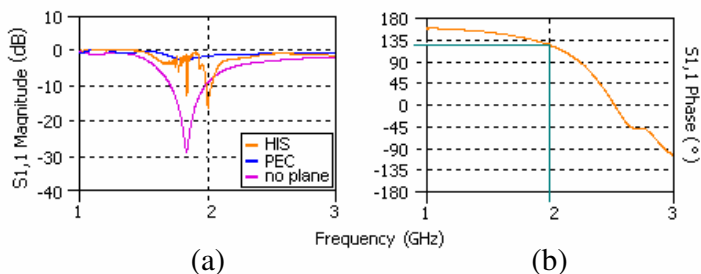


Figure 7. (a) Return loss ($|S_{11}|$) of the horizontal dipole when situated over the mushroom-like HIS. (b) Reflection phase of the mushroom-like HIS.

specially, if low profile is required. Minimum return loss of -16 dB is achieved by the horizontal dipole over the mushroom-like HIS, so it can be considered that this type of artificial ground plane is a good alternative to be used with low profile wire antennas. The -10 dB-return-loss bandwidth is 3%, which is clearly narrow band. This value is considerably smaller than the 13.25% of -10 dB-return-loss bandwidth that has the dipole in free space. Another significant point to notice is that the resonant frequency of the dipole belongs to the frequency band in which the mushroom-like HIS shows EBG behaviour (1.5 to 2.4 GHz, according to the results in Section 3). Due to this fact, as the energy loss associated to the surface waves decreases, the radiation efficiency would be higher.

Figure 7(b) shows the reflection phase of the mushroom-like HIS when considering the metallization size readjustment after designing the antenna in conjunction with the plane. The better return loss of

the horizontal dipole is obtained when the reflection phase is 127° . Consistent with the results in [17], the mushroom-like HIS requires a reflection phase in the range of $90^\circ \pm 45^\circ$ for a low profile wire antenna to obtain a good return loss.

Radiation patterns of the horizontal dipole over the mushroom-like ground plane are presented in Figure 8 for different frequency values. The reason why several frequencies have been represented is to illustrate the radiation pattern properties over a wide bandwidth.

As it can be seen, the radiation patterns obtained are quite different than those associated to the horizontal dipole over a PEC ground plane, which have peak directivity normal to the ground plane. As previously commented, when designing an antenna in conjunction with a HIS, it must be taken into account that both elements must be designed simultaneously, as a single antenna structure. Such structure has a characteristic radiation pattern, clearly affected by the strong interaction between the dipole and the HIS due to their close proximity.

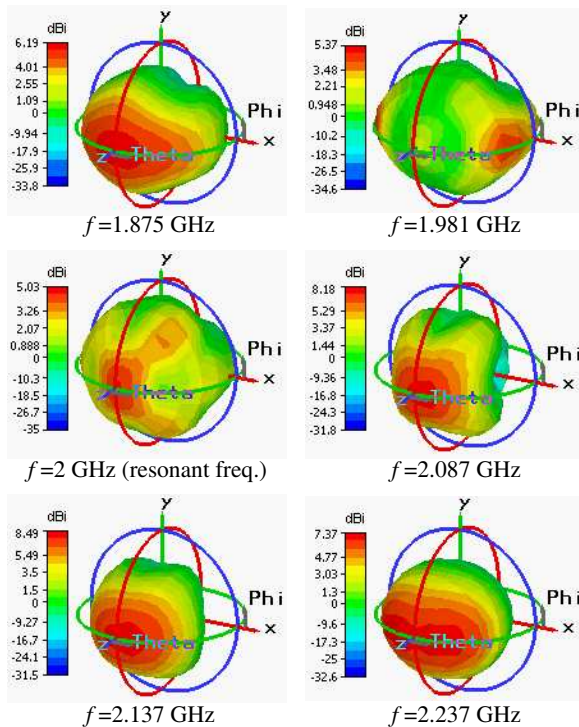


Figure 8. Radiation pattern of the horizontal dipole when situated over the mushroom-like HIS (8×8 cells).

In this specific case, such strong coupling makes radiation patterns be quite degraded. One clear example of this is the radiation pattern at the resonant frequency ($f = 2 \text{ GHz}$), in which the maximum radiation spreads from the broadside pointing direction towards the corners of the ground plane. This radiation in the corners seems to be generated within the HIS, as a surface-wave mode, and it is quite damaging because it quite increases the back radiation.

4.2. Ring Metallization Ground Plane (5×5 Unit Cells)

In the case of the horizontal dipole over the ring metallization HIS (see Figure 9), the same analysis process will be followed.

Figure 10(a) shows the return loss in the three cases under study, though we will focus on the artificial plane. When the horizontal

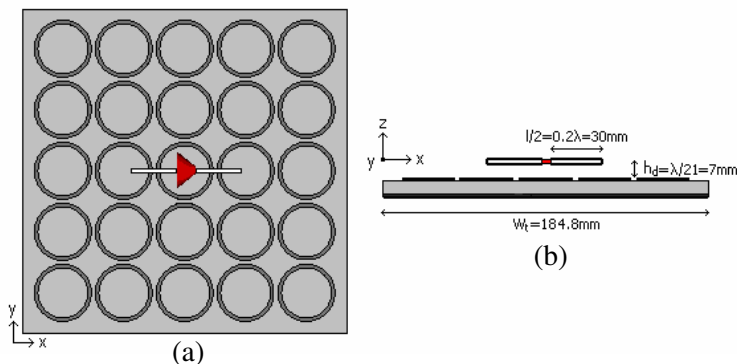


Figure 9. Horizontal dipole over ring metallization HIS. (a) Top view and (b) side view.

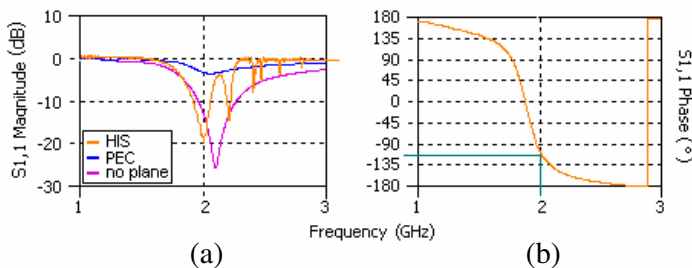


Figure 10. (a) Return loss ($|S_{11}|$) of the horizontal dipole when situated over the ring metallization HIS. (b) Reflection phase of the ring metallization HIS.

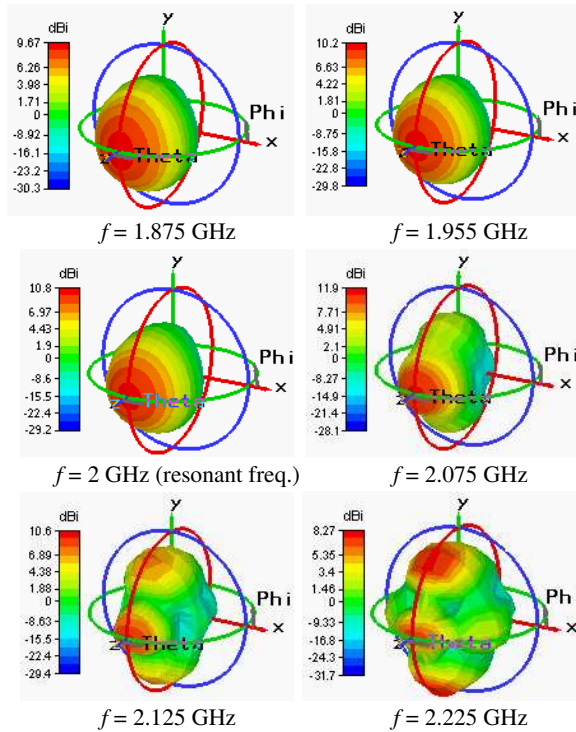


Figure 11. Radiation pattern of the horizontal dipole when situated over the ring metallization HIS (5×5 cells).

dipole is over the ring metallization HIS, the return loss is -20 dB, which is quite a good value. The -10 dB-return-loss bandwidth is 7%, which can be considered narrow band, but less than in the case of the mushroom-type. The reflection phase of the redesigned ring metallization HIS, shown in Figure 10(b), must be -112° in order to obtain a good return loss of the antenna. This criterion differs from that of the mushroom-like HIS. However, analogously to the mushroom case, it can be considered that the ring metallization HIS requires a reflection phase in the range of $-90^\circ \pm 45^\circ$ for a low profile wire antenna to obtain a good return loss. This will be clearly observed when analysing the radiation pattern.

When analysing the radiation pattern behaviour, it is necessary to keep in mind that the frequency range associated to the useful reflection phase range ($-90^\circ \pm 45^\circ$), is between 1.93 GHz and 2.1 GHz. As it can be seen in Figure 11, all radiation patterns that belong to this frequency range, are quite shaped, having almost perfect revolution symmetry.

They have peak directivity normal to the ground plane (broadside pointing direction) and negligible back radiation. On the contrary, radiation patterns in a frequency over 2.1 GHz, are quite degraded.

4.3. Open Ring Metallization Ground Plane (7 × 7 Unit Cells)

The last structure to be analysed is the one made of a horizontal dipole over an open ring metallization artificial ground plane, as represented in Figure 12.

Unlike the other dipole-HIS structures, the horizontal dipole in this case is oriented along the y -axis because matching is better than the one obtained for the dipole when oriented along the x -axis. In

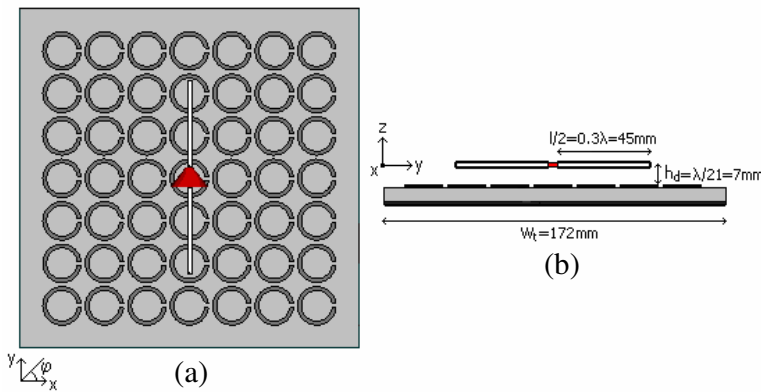


Figure 12. Horizontal dipole over open ring metallization HIS. (a) Top view and (b) side view.

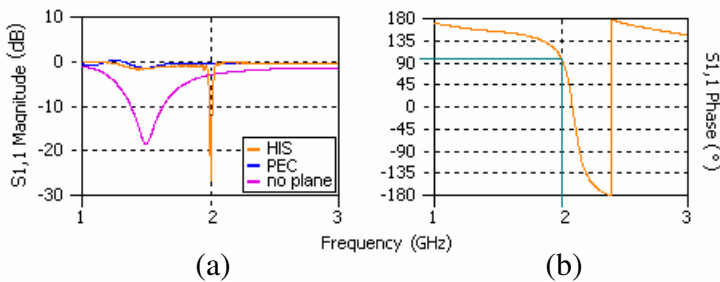


Figure 13. (a) Return loss ($|S_{11}|$) of the horizontal dipole when situated over the open ring metallization HIS. (b) Reflection phase of the open ring metallization HIS.

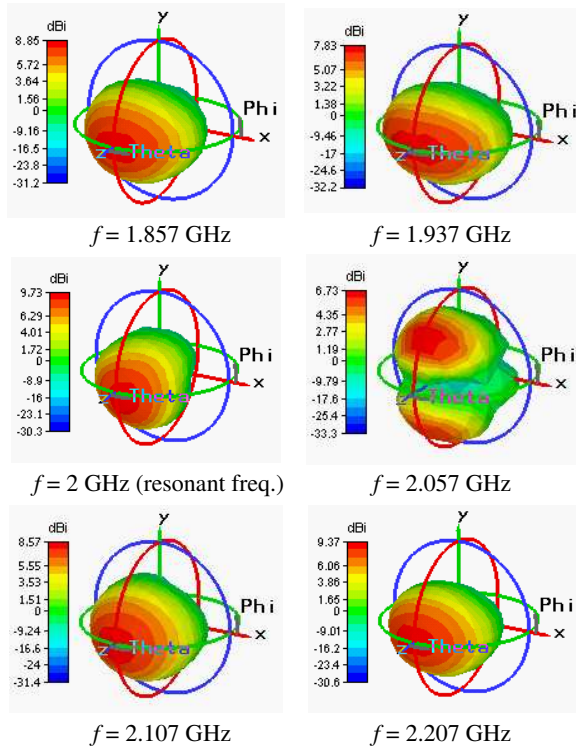


Figure 14. Radiation pattern of the y-axis-oriented horizontal dipole when situated over the open ring metallization HIS (7×7 cells).

fact, due to the asymmetry of the structure, different orientations of the dipole were studied ($\varphi = 0^\circ$, $\varphi = 45^\circ$ and $\varphi = 90^\circ$), being the y -axis orientation the one exhibiting the best performance. Concerning the design process, it is also important to highlight that, again because of the unit cells asymmetry, the antenna cannot directly match well, so it is quite difficult to design the dipole-HIS structure, and even when finally correctly designed, results are quite poor.

The horizontal dipole, in conjunction with the open ring metallization HIS, has a minimum return loss of -26.77 dB at a frequency of 2 GHz; however, the -10 dB-return-loss bandwidth is 1%, which is quite narrow. The best return loss of the horizontal dipole is obtained when the reflection phase is 115° (see Figure 13). This narrow bandwidth is not surprising as the open ring metallization structures, known as well as split ring resonators (SRR), are very narrow band.

When analysing the radiation pattern behaviour, it is easy to realize how determinant and damaging the asymmetry of the structure

is. According to the different patterns shown in Figure 14, it is clear that the behaviour is quite unexpected, as the most well shaped patterns are obtained at both the lower and upper frequencies of the band under study.

5. GROUND PLANE SIZE REDUCTION

The aim of this section is to determine the effect of reducing the HIS dimensions on the horizontal dipole radiation pattern. The structure chosen to carry out this work is the ring metallization one, as it has proven to behave better than the others, especially regarding the radiation pattern. Tables 3 and 4 summarize the results obtained in the previous section (Section 4). Concerning the matching, the ring metallization HIS shows the best -10 dB-return-loss bandwidth and a return loss value more than acceptable. Regarding the radiation pattern at the resonant frequency, it has revolution symmetry, negligible back radiation and the best gain value. These characteristics make the ring metallization HIS the most suitable structure for analysing the effect of the size reduction.

The reference structure chosen to carry out the analysis has 5 rows and 5 columns of unit cells. To reduce the plane size, the outer unit cells of the structure are sequentially removed, so that 4×4 ,

Table 3. Dipole-HIS structures — Matching.

HIS metallization	Mushroom-like	Ring	Open ring
Return loss	-16 dB	-20 dB	-26.77 dB
$BW_{-10\text{ dB}}$	3 %	7%	1%

Table 4. Dipole-HIS structures — Radiation Pattern (at resonant frequency).

HIS metallization	Mushroom-like	Ring	Open ring
Pointing direction	Broadside	Broadside	Broadside
Directivity	8.07 dBi	10.6 dBi	9.5 dBi
Tot. efficiency	0.9804	0.9853	0.8953
Gain	7.98 dBi	10.53 dBi	9.02 dBi
Back radiation	High Max. level = 0 dBi	Negligible	Medium Max. level = -11 dBi
Shape	Degraded	Revolution symmetry	Degraded

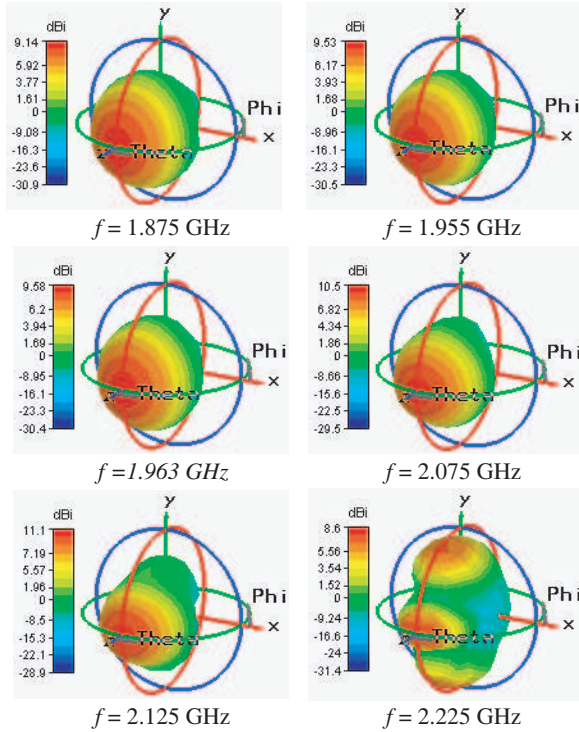


Figure 15. Radiation pattern of the horizontal dipole over the ring metallization HIS (4×4 cells).

3×3 and 2×2 unit cell planes are obtained. In order to analyse the plane reduction effect on the horizontal dipole radiation pattern, the originally designed dipole, of $0.40\lambda_{2\text{GHz}}$ length and 7 mm height in the case of the ring metallization HIS, must remain exactly the same in all cases. Although not determining to this analysis, it is important to notice that the resonant frequency of the dipole (written in italics in the following figures) changes in every case due to the different sizes of the ground plane.

Figures 15, 16 and 17 show the radiation pattern of the horizontal dipole over the ring metallization HIS, considering 4×4 , 3×3 and 2×2 unit cells respectively.

According to the figures, pattern degradation clearly occurs at upper frequencies, limiting the usable operating bandwidth. Nevertheless, as more outermost rings of the HIS are removed, less significant is the pattern degradation, even in the upper frequency band. This way, the radiation pattern of the smallest HIS (2×2

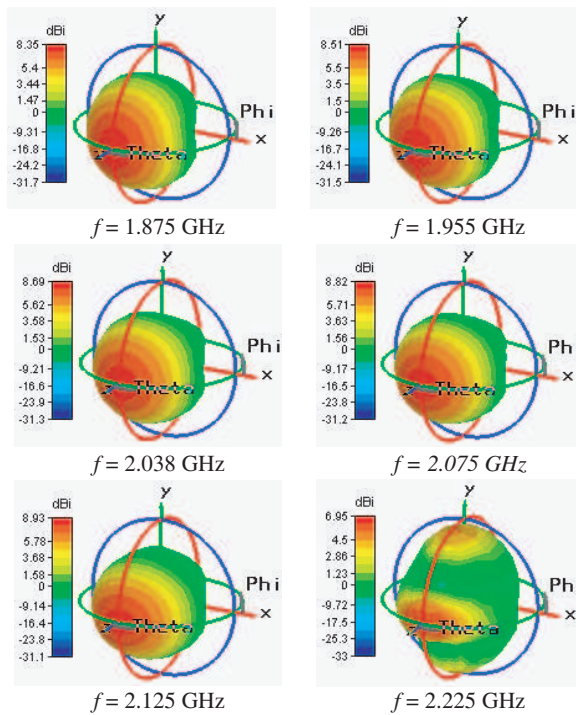


Figure 16. Radiation pattern of the horizontal dipole over the ring metallization HIS (3×3 cells).

unit cells), is quite shaped in all the frequency band under study, having almost perfect revolution symmetry in all cases. This result is quite interesting, as the smallest HIS proves to be the more stable regarding radiation pattern behaviour. Considering the importance of minimizing the size of the radiating structures in certain applications, this fact is quite revealing.

There is, however, a negative consequence of decreasing the size of the artificial ground plane. This is that the return loss of the dipole gets worse. This way, whereas a return loss around -20 dB is obtained in the cases of 4×4 and 3×3 unit cells, only -8 dB return loss is obtained in the 2×2 unit cell ground plane. Thereby, though minimizing the ground plane size is good concerning the radiation pattern behaviour, it is important not to make the plane so small as to make the dipole not to be matched.

Also, the polar E-field radiation patterns at the resonant frequency will be studied in order to determine how determinant is the ground plane size for the back radiation level. According to Figure 18, the

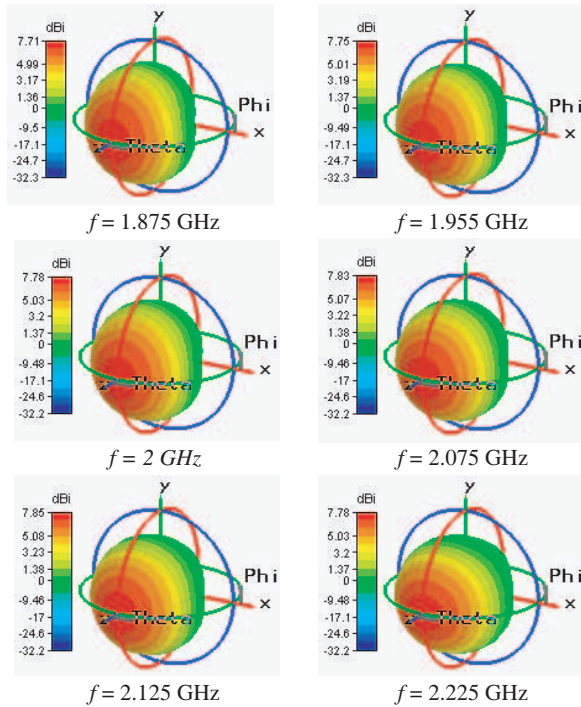


Figure 17. Radiation pattern of the horizontal dipole over the ring metallization HIS (2×2 cells).

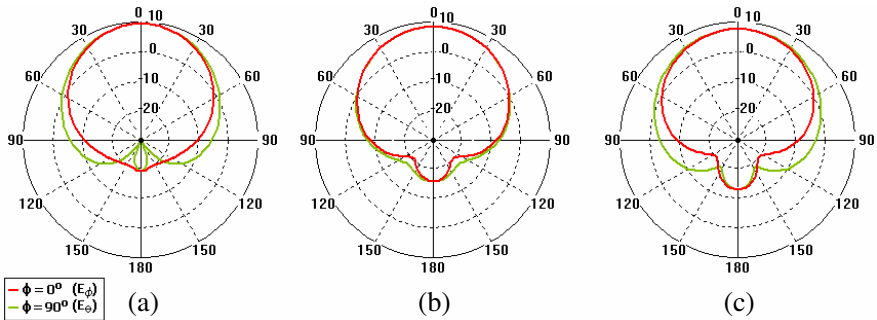


Figure 18. Simulated E-field radiation patterns of the horizontal dipole over ring metallization HIS. (a) 4×4 unit cells, (b) 3×3 unit cells and (c) 2×2 unit cells.

smaller the ground plane, the higher back radiation level. This result was expected, as smaller ground planes prevent wave radiation to propagate backwards. In spite of this, it can be considered that quite acceptable back radiation levels are obtained in the three cases under study.

Finally, in order to complete the results of this section, a quick review of the consequences of the ground plane size reduction in the cases of mushroom-like and open ring metallization HIS will be made. Although results are not included in this paper, simulations have been made in order to determine how the radiation pattern is affected when sequentially removing the outer unit cells of these two different structures. What has been observed, is that, consistent with the results of the ring metallization HIS, radiation patterns are less degraded in the lower and upper frequencies as the number of cells is reduced. Nevertheless, the improvement is not so noticeable as in the case of the ring metallization HIS.

6. EXPERIMENTAL RESULTS

In order to validate some of the results presented in this paper, all the HIS-based ground planes described in Section 4 were fabricated. Nevertheless, because of simplicity reasons, a horizontal monopole, instead of a horizontal dipole was implemented.

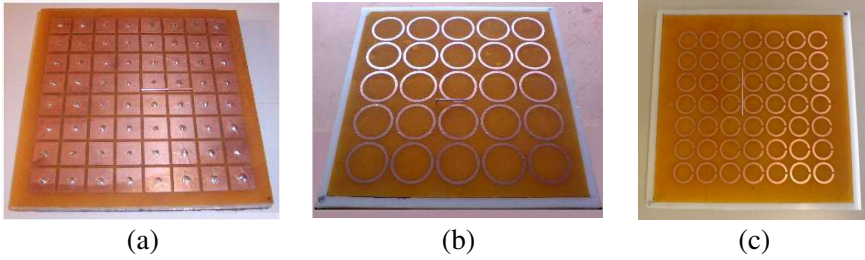
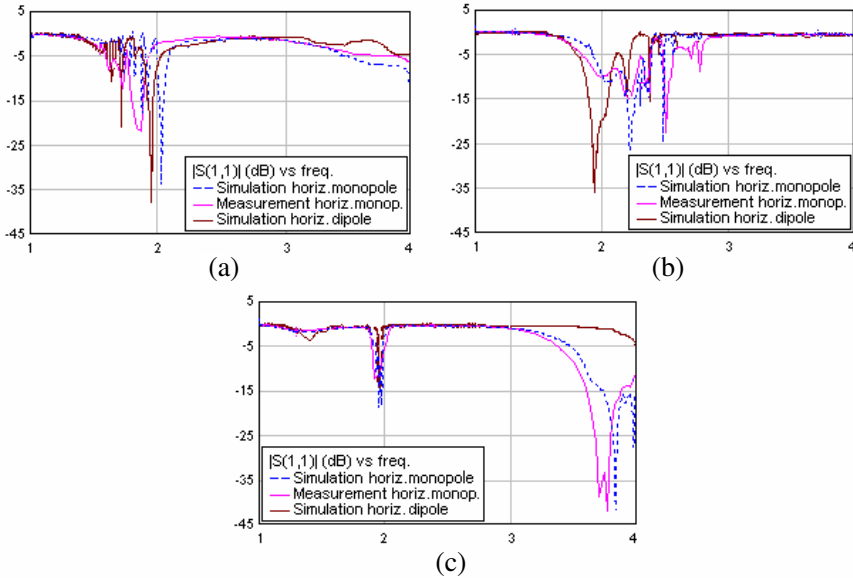
All metallizations are photoengraved on a 35 microns thick copper sheet. As to make possible the photoengraving process, a kapton sheet of 25 microns thick and dielectric constant of 3.4 is placed over a polyethylene substrate with dielectric constant of 2.2 and 5 mm thickness. The gap size is 2 mm. The mushroom-like HIS is 175.5 mm long (8 cells of 17.5 mm width plus extra distance to the edges), and has metallic vias of 0.25 mm radius. The ring metallization HIS is 187 mm long (5 cells of 32 mm width plus extra distance to the edges), with rings of 2 mm width. Finally, the open ring metallization HIS is 176 mm long (7 cells of 20 mm width plus extra distance to the edges), with rings of 2 mm width opened an angle of 10° . The dimensions of the horizontal monopole in all three cases under study are shown in Table 5 and photographs of all horizontal monopole-HIS structures can be seen in Figure 19.

The simulated and measured return losses ($|S_{11}|$) of the three HIS based ground planes, of both the horizontal dipole and monopole antennas are plotted in Figure 20.

As it can be observed, the wire antennas on all ground planes are well matched with return losses below -10 dB, so most of the power is radiated. The resonant frequency of the simulation is 2 GHz in all

Table 5. Horizontal monopole dimensions.

Metallization	Length	Height
Mushroom	$0.237\lambda_{2\text{GHz}} = 35.5 \text{ mm}$	$0.033\lambda_{2\text{GHz}} = 5 \text{ mm}$
Ring	$0.17\lambda_{2\text{GHz}} = 25.5 \text{ mm}$	$0.027\lambda_{2\text{GHz}} = 4 \text{ mm}$
Open Ring	$0.30\lambda_{2\text{GHz}} = 45 \text{ mm}$	$0.047\lambda_{2\text{GHz}} = 7 \text{ mm}$

**Figure 19.** Horizontal monopole over HIS. (a) Mushroom-like, (b) ring metallization and (c) open-ring metallization.**Figure 20.** Simulated and measured horizontal wire antennas return losses. (a) Mushroom-like HIS, (b) ring metallization HIS and (c) open ring metallization HIS.

cases, practically the same as that of the measurement, with a good agreement.

7. CONCLUSIONS

Three different types of high impedance surfaces have been investigated and compared: a mushroom-like HIS, a ring metallization HIS and an open ring metallization one, which is anisotropic. Many other planar unit cells can be studied for the same application, as those proposed in [16, 18] or the Jerusalem Cross. Among all possibilities, these three were chosen because of their simplicity and representativeness.

Regarding the ground planes characteristics, it has been verified that the desired behaviour is successfully accomplished in all cases as demonstrates the fact that a horizontal dipole can be matched even when extremely close to the ground plane. The horizontal wire antennas placed above the three HIS are well matched with return losses below -10 dB and it can be said that they radiate very well in contrast to those above conventional metal ground planes.

The best results have been obtained for the ring metallization HIS both in terms of bandwidth and radiation pattern. Also, very good return loss and gain values have been achieved. The bandwidth is given by the smooth variation of the reflection phase with the frequency. Treating the unit cell as a resonator, this means that the ring cell is less resonating than the other two. Another advantage is that, in spite of the fact that the ring unit cell is the least compact of the three, not many cells are necessary to make the antenna be matched. Furthermore, this structure is the one that provides the best radiation pattern behaviour, being the rotational symmetry good for the radiation properties. It is also quite simple and cheap to fabricate as it is totally planar.

ACKNOWLEDGMENT

Part of this work was funded by ‘COMUNIDAD DE MADRID/UNIVERSIDAD CARLOS III DE MADRID’ under Project CCG10-UC3M/DPI-5631.

REFERENCES

1. Ziolkowski, R. W. and E. Heyman, “Wave propagation in media having negative permittivity and permeability,” *Physical Review E*, Vol. 64, No. 5, 056625, Oct. 2001.

2. Shelby, R. A., D. R. Smith, and S. Schultz, "Experimental verification of a negative refractive index of refraction," *Science*, Vol. 292, 77–79, Apr. 2002.
3. Yang, F. and Y. Rahmat-Samii, *Electromagnetic Band Gap Structures in Antenna Engineering*, Cambridge University Press, New York, 2009.
4. Oraizi, H. and A. Abdolali, "Some aspects of radio wave propagation in double zero metamaterials having the real parts of epsilon and mu equal to zero," *Journal of Electromagnetic Waves and Applications*, Vol. 23, No. 14–15, 1957–1968, 2009.
5. Zhou, H., S. Qu, Z. Pei, Y. Yang, J. Zhang, J. Wang, H. Ma, C. Gu, X. Wang, Z. Xu, W. Peng, and P. Bai, "A high-directive patch antenna based on all-dielectric near-zero-index metamaterial superstrates," *Journal of Electromagnetic Waves and Applications*, Vol. 24, No. 10, 1387–1396, 2010.
6. Goussetis, G., A. P. Feresidis, and J. C. Vardaxoglou, "Tailoring the AMC and EBG characteristics of periodic arrays printed on grounded dielectric substrate," *IEEE Transactions on Antennas and Propagation*, Vol. 54, No. 1, 82–89, January 2006.
7. Aminian, A., F. Yang, and Y. Rahmat-Samii, "In-phase reflection and EM wave suppression characteristics of electromagnetic band gap ground planes," *IEEE Antennas and Propagation Society International Symposium*, Ohio, 2003.
8. Hansen, R. C., "Effects of a high-impedance screen on a dipole antenna," *IEEE Antennas and Wireless Propagation Letters*, Vol. 1, 46–49, 2002.
9. Yousefi, L., H. Attia, and O. M. Ramahi, "Broadband experimental characterization of artificial magnetic materials based on a microstrip line method," *Progress In Electromagnetics Research*, Vol. 90, 1–13, 2009.
10. De Cos, M. E., Y. Alvarez, and F. Las-Heras, "Planar artificial magnetic conductor: Design and characterization setup in the RFID SHF band," *Journal of Electromagnetic Waves and Applications*, Vol. 23, No. 11–12, 1467–1478, 2009.
11. Sievenpiper, D., "High-impedance electromagnetic surfaces," Ph.D. Dissertation, University of California, Los Angeles, 1999.
12. Sievenpiper, D., L. Zhang, R. F. J. Broas, N. G. Alexopolous, and E. Yablonovitch, "High-impedance electromagnetic surfaces with a forbidden frequency band," *IEEE Transactions on Microwave Theory and Techniques*, Vol. 47, No. 11, 2059–2074, 1999.
13. Zhang, Y., B. Z. Wang, W. Shao, W. Yu, and R. Mittra, "Artificial

- ground planes for performance enhancement of microstrip antennas,” *Journal of Electromagnetic Waves and Applications*, Vol. 25, No. 4, 597–606, 2011.
14. Feresidis, A. P., G. Goussetis, S. Wang, and J. C. Vardaxoglou, “Artificial magnetic conductor surfaces and their application to low-profile high-gain planar antennas,” *IEEE Transactions on Antennas and Propagation*, Vol. 53, No. 1, 209–215, Jan. 2005.
 15. Zhang, Y., J. von Hagen, M. Younis, C. Fischer, and W. Wiesbeck, “Planar artificial magnetic conductors and patch antennas,” *IEEE Transactions on Antennas and Propagation*, Vol. 51, No. 10, 2704–2712, Oct. 2003.
 16. Sohn, J. R., K. Y. Kim, H. S. Tae, and H. J. Lee, “Comparative study on various artificial magnetic conductors for low-profile antenna,” *Progress In Electromagnetics Research*, Vol. 61, 27–37, 2006.
 17. Yang, F. and Y. Rahmat-Samii, “Reflection phase characteristics of the EBG ground plane for low profile wire antenna applications,” *IEEE Transactions on Antennas and Propagation*, Vol. 51, No. 10, 2691–2703, Oct. 2003.
 18. De Cos, M. E., Y. Alvarez Lopez, R. C. Hadarig, and F. Las-Heras Andrés, “Flexible uniplanar artificial magnetic conductor,” *Progress In Electromagnetics Research*, Vol. 106, 349–362, 2010.